TOR kinase controls *Arabidopsis* shoot development by translational repression of cytokinin catabolic enzymes

Denis Janocha[1], Anne Pfeiffer[1,2], Yihan Dong[3], Ondřej Novák[4], Miroslav Strnad[4], Lyuba A Ryabova[3] & Jan U. Lohmann[1]*

[1]Department of Stem Cell Biology, Centre for Organismal Studies, Heidelberg University; D-69120 Heidelberg, Germany

[2]current address: Bayer AG, Crop Science Division, Alfred-Nobel-Str. 50, 40789 Monheim am Rhein, Germany

[3]Institut de biologie de moléculaire des plantes UPR2357 du CNRS, Université de Strasbourg, Strasbourg, France

[4]Laboratory of Growth Regulators, Institute of Experimental Botany, The Czech Academy of Sciences and Faculty of Science, Palacký University, Šlechtitelů 27, 78371, Olomouc, Czech Republic

*corresponding author

Mailing address of corresponding author:

Jan U. Lohmann
Centre for Organismal Studies
Department of Stem Cell Biology
Heidelberg University
Im Neuenheimer Feld 230
D-69120 Heidelberg
Germany

PH: +49 6221 546269
FX: +49 6221 546424
EM: jan.lohmann@cos.uni-heidelberg.de

Abstract

Plants continuously adjust organ initiation and growth to endogenous and environmental signals. At the heart of this postembryonic mode of development are stem cells, whose activity is influenced by a large diversity of signaling pathways. We have shown previously that the TARGET OF RAPAMYCIN (TOR) kinase network controls expression of *WUSCHEL (WUS)*, a transcriptional master regulator of stem cells in the shoot apical meristem (SAM), by integrating metabolic- and light signals. While this provided a framework how environmental parameters determine shoot development, the mechanisms linking TOR and *WUS* activity remained unresolved. Here we show that TOR controls the accumulation of *trans*-zeatin, the cytokinin species mainly responsible for shoot development, by translational repression of RNAs encoding cytokinin degrading CYTOKININ OXIDASES/DEHYDROGENASE (CKX) enzymes. Thus, our work not only sheds light on how plants are able to quickly adjust stem cell activity in response to their environment, but also opens new avenues for studying the mechanisms translating TOR kinase activity into relevant biological output.

Introduction

Due to their sessile life-style, plants need to dynamically adjust organ development and growth in response to variable environmental conditions. Therefore, they are able to integrate diverse local and systemic signals to adjust stem cell behavior accordingly. Stem cells of the SAM are controlled by the activity of the homeodomain transcription factor WUS (Bäurle & Laux, 2005; Daum et al., 2014; Laux et al., 1996; Mayer et al., 1998; Schoof et al., 2000) and previous studies have shown that *WUS* expression is modulated in response to environmental signals such as nitrate availability or the current light- and energy regime (Janocha & Lohmann, 2018; Landrein et al., 2018; Li et al., 2017; Pfeiffer et al., 2016). In the absence of a neuronal system, plants make use of complex hormone signaling systems for long distance information relay. Among those, cytokinins (CKs) and particularly *trans*-zeatin (*tZ*), are involved in nitrate and light signaling from root and leaves to the SAM, respectively (Landrein et al., 2018; Yoshida et al., 2011). CKs in turn promote *WUS* expression, thus tuning stem cell number in response to the environment (Buechel et al., 2010; Gordon et al., 2009; Kiba et al., 2013; Landrein et al., 2018; Osugi et al., 2017).

CK homeostasis is controlled by tightly regulated biosynthesis and degradation systems (Heyl et al., 2018), with ISOPENTYLTRANSFERASES (IPTs) catalyzing the first step in the anabolic pathway. IPT enzymes synthesize isopentyladenosine-5´-monophosphate (iPRMP) precursors, which can be hydroxylated by CYP735A1/2 to obtain *trans*-zeatin riboside-5´-monophosphate (tZRMP). Both precursors are then converted by so called LONELY GUY (LOGs) enzymes to obtain the active nucleobases isopentyladenin (iP) and *tZ* (Kuroha et al., 2009). CK degradation in *Arabidopsis* is mediated by seven CYTOKININ OXIDASE / DEHYDROGENASE (CKX) enzymes, which are characterized by distinct tissue specific expression patterns making them important players to locally and globally control CK signaling activity (Bartrina et al., 2011; Holst et al., 2011; Köllmer et al., 2014; X. Wang et al., 2020; Werner et al., 2003). Intracellular CK signal transduction is based on a two-component phospho-relay (Kieber & Schaller, 2014). The receptors are *ARABIDOPSIS HISTIDINE KINASES* (*AHK*s) and likely reside on the plasma membrane and the endoplasmic reticulum (Antoniadi et al., 2020). Upon CK binding, AHKs auto-phosphorylate and then pass on the phosphoryl group to *ARABIDOPSIS HISTIDINE PHOPHOTRANSFER PROTEINS* (*AHP*s). AHPs continuously shuttle between cytoplasm and nucleus where they interact with and activate type-B *ARABIDOPSIS RESPONSE REGULATORS* (*ARR*s) transcription factors by phosphorylation (Kieber & Schaller, 2014). These regulators induce expression of CK response genes, including type-A *ARR*s, which in turn dampen the CK response in a negative

feedback system. Since type-A *ARR*s are primary CK response genes and activated within minutes of treatment, their expression serves as a proxy for CK pathway output. In addition, several other genes encoding enzymes involved in CK biosynthesis or degradation are among the CK response genes, resulting in complex, tissue specific feed-back systems.

While continuously active stem cells only contribute to postembryonic development of plants, apical meristems are set up and defined during embryogenesis, but remain inactive until germination. We showed previously that during germination, *WUS* expression is synergistically controlled by photoreceptor-mediated light signaling and photosynthesis derived sugars and that both pathways require activity of the TOR kinase (Pfeiffer et al., 2016). TOR is an evolutionary conserved regulator of growth and acts as central nutrient sensor promoting anabolic processes, like protein biosynthesis under favorable conditions, while at the same time limiting autophagy driven catabolic turnover (G. Y. Liu & Sabatini, 2020; Shi et al., 2018; Tafur et al., 2020). By phosphorylation of central regulators of ribosome biogenesis and cell cycle regulation, such as S6K1 and E2FA, TOR controls transcriptome and metabolic reprogramming to facilitate adaptation to changes in energy- and nutrient availability (Y. Dong et al., 2017; Xiong et al., 2013). Although much progress has been made in elucidating the TOR signaling landscape in mammals, our understanding of the TOR network in plants remains relatively poor. Recently, it has been demonstrated that TOR dependent phosphorylation of ETHYLENE INSENSITVE 2 (EIN2) controls growth of etiolated seedlings and mediates the transcriptional response to glucose in an ethylene independent manner (Fu et al., 2021). Moreover, the phytohormones auxin and abscisic acid have been identified as upstream regulators that influence TOR activity by modulating complex assembly with the associated regulatory protein RAPTOR (Li et al., 2017; P. Wang et al., 2018).

Whereas the mechanisms connecting TOR with sugar and hormone responses have begun to emerge, little is known about how TOR controls shoot growth and SAM activity. We showed previously that TOR dependent stem cell activation correlated with increased CK signaling in the SAM and that mutations in *ckx5* and *ckx6* promoted *WUS* expression during germination. However, the mechanisms connecting TOR kinase and CK signaling had remained elusive. Here, we report that for *WUS* expression and shoot development, the cytokinin *tZ* is the most relevant downstream effector of TOR and demonstrate that translational regulation of cytokinin catabolic enzymes represents a major mechanism for TOR kinase to control *tZ* levels.

Results

The transcriptional response to TOR inhibition in *Arabidopsis* shoots

Building on our previous results that demonstrated that TOR acts as the central integrator of light and sugar signaling during stem cell activation (Pfeiffer et al., 2016), we set out to identify downstream regulatory pathways that connect TOR with *WUS* expression and shoot development. Therefore, we analyzed the transcriptomes of *Arabidopsis* shoots with impaired TOR function. Because *tor null* mutants are lethal (Menand et al., 2002) and *Arabidopsis* is insensitive to Rapamycin, we applied short term treatments with three independent TOR active site inhibitors, namely AZD8055, TORIN1 and KU63794 (Q. Liu et al., 2012; Montané & Menand, 2019; Schenone et al., 2011). We chose working concentrations (2 μM AZD8055, 10 μM TORIN1, 10 μM KU63794) that have been shown to substantially impair shoot growth (P. Dong et al., 2015) and determined the earliest time point these inhibitors showed a robust effect on TOR activity in seedling shoots using S6K1 phosphorylation as a readout (Fig. S1). We observed robust reduction of S6K1 phosphorylation in shoots of four days old seedlings eight hours after transfer to 2 μM AZD8055 and 10 μM TORIN1 but not for 10μM KU63794. We therefore tested KU63794 at 20 μM, which indeed led to substantially reduced S6K1 phosphorylation after 8h (Fig. S1). Using these experimental parameters along with RNA-seq, we were able to identify the expression of 23654 genes across all samples. Using DESeq2 (Love et al., 2014), we found 6639 differentially expressed genes (DEGs) in inhibitor treated samples compared to the mock control (Fig. 1a + Table S1), among which 3266 (49.2%) showed reduced expression, whereas 3373 (50.8%) transcripts accumulated to higher levels than in controls. Most genes were affected by AZD8055 (5303 DEGs) followed by KU63794 (4556 DEGs) and TORIN1 (3692 DEGs). The different treatments caused significantly overlapping effects, with 2509 (37.7%) DEGs common to all three inhibitors and 4403 (66.3%) DEGs found in at least two of three treatments, suggesting that we were able to identify a robust set of TOR sensitive transcripts. The differences between the inhibitors are likely due to unique selectivity-, potency and efficacy profiles of the three substances (Q. Liu et al., 2012; Montané & Menand, 2019; Schenone et al., 2011). Comparisons with previously published RNAseq data revealed significant overlap with studies using AZD8055 (P. Dong et al., 2015) or TORIN2 (Scarpin et al., 2020) as inhibitors (Fig. S2), even though the experimental setup utilized differed substantially from ours. The overlap in DEGs compared with microarray data of RNAi lines against TOR three and six days after induction was rather mild (Caldana et al., 2013), which was expected given the highly divergent experimental setup.

For further analysis we focused on mRNAs that showed a similar behavior in response to at least two inhibitors (significant difference in abundance with the same direction of change),

which resulted in 4398 high confidence TOR target genes (Fig. 1a + Table S1). We chose to not apply any expression cut off because the genes selected were behaving consistently in at least six to nine replicates, rendering them interesting targets for investigation even if the fold change may be fairly low. Among the genes with reduced expression, GO categories (Table S1) of well characterized TOR dependent processes were most prevalent, such as translation, ribosome biogenesis, tRNA metabolism and anabolic processes (Dobrenel et al., 2016; Shi et al., 2018). The same applied to transcripts with increased accumulation among which we found GO categories (Table S1) related to catabolism, autophagy, secondary metabolism, glucosinolate biosynthesis and photosynthesis to be enriched (P. Dong et al., 2015; Malinovsky et al., 2017; Pu et al., 2017; Ren, 2015; Scarpin et al., 2020).

During detailed inspection of our data, we identified also many DEGs with annotations related to hormone signaling pathways (Fig. 1b + Table S1) with genes related to abscisic acid (ABA) but also auxin, cytokinins (CKs), jasmonic acid (JA), ethylene, brassinosteroids (BR) and gibberellic acid (GA) being well represented. Interestingly, for most hormones the number of transcripts showing increased or reduced levels were similar. Notable exceptions were CKs and jasmonic acid, where the abundance of most transcripts was reduced in response to TOR inhibition. This apparent reduction of pathway activity caught our attention because of the known positive effect of CKs on SAM activity and shoot development (Kiba et al., 2013; Osugi et al., 2017). The transcriptome analysis revealed differential regulation of genes involved in CK biosynthesis (*IPT1, -9. CYP735A2, LOG5, -8*), -transport (*PUP1, -14*), -sensing (*AHK4*), -signal transmission (*AHP1, -2*) and -transcriptional regulation (*ARR2, -10, -14*) (Fig. 1c). Notably, all six type-A *ARRs* that appeared as differentially regulated in our dataset were repressed after inhibitor treatment. Expression of type-A *ARRs* is commonly used as an approximation for CK signaling output and we thus concluded that CK signaling response is likely reduced following TOR inhibition.

TOR inhibition reduces cytokinin signaling in the SAM

To test whether our findings obtained at the level of the entire seedling shoot bear any relevance for the SAM, we used the well-established *pTCSn:GUS* CK signaling reporter line (Zürcher et al., 2013). Supporting the RNA expression data for type-A *ARRs*, we found that *pTCSn* activity was substantially reduced after AZD8055 treatment especially in the meristematic region of the shoot, where CK function is required to maintain *WUS* expression (Fig. 1d+e + Fig. S3). We next asked whether the reduction in CK signaling would also affect *WUS* expression. To this end, we utilized our previously established *pWUS:3xVenus:NLS* transcriptional reporter system (Pfeiffer et al., 2016). Importantly, we investigated etiolated

seedlings, since in their SAMs *WUS* is usually not expressed, giving us a maximum of sensitivity to test different stimuli for their ability to activate *WUS*. In addition, we have previously shown that the CK 6-benzyladenin (6-BA) is able to induce *WUS* expression in this setting (Pfeiffer et al., 2016), allowing us to quantitatively test the effect of TOR inhibition on CK dependent activation of *WUS*. Indeed, CK dependent activation of *WUS* was almost fully blocked when 6-BA was applied together with AZD8055 (Fig. 2a). Consistently, 6-BA induced expression of several type-A *ARRs* was suppressed when seedlings were preincubated with the TOR inhibitor (Fig. S4). Together, this suggested that TOR inhibition interferes with the activation of various CK response genes in the SAM, including *WUS*.

Since reduced CK signaling could be a major cause for the previously observed effects of TOR inhibition on SAM activity and *WUS* expression, we next aimed at identifying at which step of the pathway this effect may occur. Transcription factors of the type-B ARRs family have been shown to directly bind to the *WUS* promoter and induce *WUS* expression in response to CK sensing (Dai et al., 2017; Gruel et al., 2016; Meng et al., 2017). To test the functional interaction between TOR and type-B ARRs for *WUS* activation, we crossed our *pWUS:3xVenus:NLS* reporter with a line carrying an inducible version of a constitutively active allele of ARR1 (*p35S:ARR1ΔDDK:GR*). In this allele, the ARR1 transcription factor was lacking the receiver domain (*ΔDDK)*, making it independent of CK induced phosphorylation. In addition, it was fused to a glucocorticoid receptor (GR) domain, enabling dexamethasone (DEX) dependent nuclear translocation and thus experimental induction (Sakai et al., 2001b). Finally, the fusion protein was expressed *in planta* from a strong and ubiquitously active viral promoter (*p35S*). Upon DEX treatment of *p35S:ARR1ΔDDK:GR* shoots, *WUS* became expressed in most cells (Fig. 2b+c+d + Fig. S5) confirming that it is a direct type-B ARR target gene. Interestingly, treatment with AZD8055 did not interfere with this response, indicating that TOR interacts with CK signaling upstream of type-B ARRs. Moreover, we found that ARR1ΔDDK mediated induction of type-A *ARR* expression was not affected by TOR inhibition (Fig. S6), supporting our conclusion.

To further narrow down the intersection of TOR kinase activity and CK signaling, we assessed whether seedlings would still be able to respond to treatment with various endogenous CK species after TOR inhibition. We therefore performed CK response assays, using *trans*-zeatin (*tZ*) and isopentyladenin (iP) as cytokinins, mRNA levels of *ARR5* as readout, and the CK receptor double mutant *cre1-2/ ahk3-7,* which is insensitive to *tZ* and *i*P, as negative control (Riefler et al., 2006) (Fig. 2e+f). Moreover, we decided to include roots in our assay system since *i*P and *tZ* are known to evoke different responses in shoots and roots, respectively. To

resolve subtle differences in CK sensing and response we decided to use moderate CK concentrations with 100 nM *t*Z and *i*P.

Application of *t*Z to wild-type seedlings evoked a strong increase of *ARR5* expression compared to the *cre1-2/ ahk3-7* mutant indicating a solid experimental baseline (Fig. 2e+f). Interestingly, when seedlings were pre-incubated with AZD8055, hardly any difference in *ARR5* expression compared with the *cre1-2/ ahk3-7* mutant was observed (Fig. 2e+f), suggesting that TOR activity is essential for transcriptional responses to exogenously applied *t*Z. Interestingly, treatment with the CK derivative *i*P had different effects. Whereas shoots seemed to be generally insensitive to this concentration of *i*P (Fig. 2f), wt roots showed solid *ARR5* accumulation compared to the *cre1-2/ ahk3-7* mutant (Fig. 2e). Notably, treatment with AZD8055 did not interfere with this response, suggesting that seedlings are in principle still able to sense CKs after TOR inhibition. Since CRE1 and AHK3 CK receptors have higher affinities towards *t*Z than *i*P (Romanov et al., 2006), it appeared unlikely that the differential response observed after TOR inhibition could arise at the receptor or the signal transduction level.

Reducing TOR activity affects cytokinin homeostasis

Our finding that seedlings are only selectively able respond to treatments with individual CK species suggested that TOR may have an effect on their accumulation either by degradation or sequestration. We therefore used metabolite analyses to quantify the *in planta* levels of CK molecules in response to TOR inhibition and found drastic changes in CK homeostasis following AZD8055 treatment (Fig. 3). For *i*P, levels of active bases were increased two-fold, whereas the monophosphate precursor (*i*PRMP) was slightly reduced. The changes in *t*Z species were even more pronounced, and we observed a reduction of active *t*Z bases to 50% of the mock levels after AZD8055 treatment. Moreover, a four-fold decrease of *trans*-zeatin riboside (*t*ZR) and a six-fold decrease of the monophosphate precursor (*t*ZRMP) occurred in response to TOR inhibition, whereas the conjugated glycosides (*t*ZOG, *t*Z7G, *t*Z9G) were almost unchanged for both *t*Z and *i*P derivatives. Importantly, *t*Z and *t*ZR have been shown to be the main CK species driving shoot development and *WUS* expression (Kasahara et al., 2004; Kiba et al., 2013; Landrein et al., 2018; Osugi et al., 2017). Thus, the drastic reduction in *t*Z and *t*ZR levels following TOR inhibition fitted well with effects of TOR activity on *WUS*. Strikingly, *cis*-zeatin (*c*Z) active bases were increased six-fold as well as all other *c*Z derivatives (Fig. 3). However, *c*Z does not show relevant CK activity in classical bioassays (Gajdošová et al., 2011; Kasahara et al., 2004) and in line with this it had very little effect on our *WUS* reporter in etiolated seedlings compared with *t*Z and *i*P (Fig. S7).

Cytokinin and sugars act downstream of TOR

Based on the striking differential accumulation of *tZ* and iP after TOR inhibition and the divergent potential of these molecules to trigger CK responses when applied at moderate concentrations in the presence of AZD8055, we hypothesized that TOR controls shoot development via the regulation of *tZ* levels. We reasoned that if reduced *tZ* levels were causal for the reduced *WUS* expression observed under TOR inhibition, exogenous re-supplementation with high concentrations of CK species should be able to rescue *WUS* promoter activity. Indeed, when we supplemented AZD8055 treated seedlings with 0.5 μM of different CKs, we observed that only *tZR*, the synthetic CK 6-BA and to a lesser extent also *tZ* were able to rescue *WUS* expression under TOR inhibition (Fig. 4a-e). This was in agreement with previous studies, showing that *tZR* and 6-BA have stronger potential to induce *WUS* and shoot development compared to *tZ* (Landrein et al., 2018; Osugi et al., 2017). However, at higher concentrations also *iP* reverted *WUS* expression to wt levels (Fig. S8).

Interestingly, this behavior was different to the one observed during stem cell activation in dark grown seedings, where 6-BA induced *WUS* expression was suppressed when TOR is inhibited (Fig. 2a). We therefore hypothesized that reduced availability of photoassimilates might be responsible for the different results obtained with etiolated seedlings. Indeed, when we supplied sugar together with 6-BA or *tZ* under TOR inhibitory conditions in dark grown seedlings, *WUS* expression was elevated to levels even higher than with 6-BA alone (Fig. 4f+g). This result was striking, since it implied that while TOR is the central gatekeeper for light-, sugar- or CK dependent activation of *WUS*, respectively, once sugars and CK act together, they are sufficient to drive *WUS* expression downstream of TOR activity. Noteworthy, the effect of sucrose alone varied between the experiments, but was not significantly different compared to *tZ*+AZD+Sucrose ($p = 0.2$, Students t-test). In sum, our results so far demonstrated that TOR inhibition leads to strongly reduced *tZ* content in shoots, which in turn is causal for reduced expression of *WUS*.

Since the relationship between TOR and *WUS* appeared to be mainly governed by *tZ* availability, we next wanted to identify the mechanisms underlying differential *tZ* accumulation. The observed reduction of *tZ* derivatives could be the result of either reduced biosynthesis or increased turnover, however our data so far clearly supported regulation by degradation. First, while expression of the gene encoding the *tZ* synthesis enzyme *CYP735A2* (Takei et al., 2004) was substantially reduced following AZD8055 treatment (Fig. 1c, Table S1), it has been shown that *CYP735A1* acts fully redundantly with *CYP735A2* and that both isoforms alone are sufficient for pathway activity (Kiba et al., 2013). Second, inhibition of the biosynthesis pathway

at various steps should lead to clearly identifiable footprints in the accumulation patterns of the diverse CK species. However, we did not observe any change that would be consistent with such footprint: A simple biosynthetic shift between *i*P and *tZ* species appeared unlikely since the increase of *i*P after inhibition was in the range of 5 pmol/mg FW whereas *tZ* reduction was about 15 pmol/mg FW. In addition, *i*PRMP levels decreased following AZD8055 treatment (Fig. 3b) despite the fact that conversion from *i*P to *tZ* happens mostly at the precursor level, since CYP735A highly favors *i*PRMP as a substrate and has only has very low affinity towards *i*P (Takei et al., 2004). The interconversion from *tZ* to *cZ* appeared equally unlikely, since the increase of *cZ* compounds is much higher than the decrease of corresponding *tZ* compounds and the existence of a *cis-trans* isomerase in plants has not been shown (Hluska et al., 2017; Miyawaki et al., 2006). Third and most importantly, AZD8055 treated shoots showed impaired response to application of moderate levels of CKs only (Fig. 2e+f), clearly pointing towards increased *tZ* turnover after TOR inhibition.

TOR activity controls cytokinin turnover via CKX enzymes

To test our hypothesis that TOR controls shoot development and *WUS* activity via CK turnover, we decided to investigate the role of CKX cytokinin degrading enzymes. To this end, we employed shoot fresh weight analyses as a quantitative proxy for shoot development in response to treatment with increasing concentrations of AZD8055. These simple assays allowed us to determine effective doses for growth inhibition (ED) across a range of genotypes and revealed that CKX enzymes are at least partially responsible for the observed effect of TOR on cytokinin mediated growth control (Fig. 5a+c+e, Fig.S9-S15). First inspection of the dose response curves suggested that wild type seedlings were more sensitive to low concentrations of AZD8055 compared with the *ckx* mutant seedlings, whereas in the higher concentration range the curves seemed to converge (Fig. 5a+e). Statistical analyses revealed that shoot fresh weight of wt seedlings differed significantly between 0 and 0.5 μM AZD8055 and also between 0.1 and 0.5 μM AZD indicating that its growth inhibitory effect set in between 0.1 and 0.5 μM (Fig. S10+S12). In contrast, shoot fresh weight for *ckx3*, *ckx4*, *ckx5* and *ckx6* mutant seedlings did not differ significantly between 0 and 0.5 μM but was only different between 0.5 and 1 μM, suggesting that growth inhibition for these mutants exclusively occurred above 0.5 μM AZD8055. Interestingly, *ckx2* and *ckx5/6* double mutants appeared to behave largely like wt seedlings.

These observations were well reflected by the different ED values for each genotype (Fig. 5f + Fig. S14). AZD8055 concentrations required to achieve 10% (ED10) or 30% (ED30) growth inhibition were substantially higher for most *ckx* mutants compared to wt except for *ckx5/6*

double mutants. Importantly, we observed a clear gradient in the difference between wt and *ckx* mutants along increasing AZD8055 concentrations with ED10 values between two to five-fold higher in mutants compared to wt, ED30 values increased up to three-fold, and ED50 values around two-fold increased. Reassuringly, these differences in ED values were statistically significant apart from *ckx2* single and *ckx5/6* double mutants. (Fig 5f). In contrast, the concentrations required to achieve 70% or 90% (ED70, ED90) growth inhibition did not differ between wild-type and mutant seedlings (Fig. S14), supporting the notion that specific *ckx* mutations render the seedlings resistant to reduction of TOR activity, but not to full inhibition.

Taken together, these experiments suggested that multiple CKX enzymes were likely to contribute to the effect of TOR on CK signaling. Importantly, this notion was also supported by experiments employing the general CKX inhibitor INCYDE (Zatloukal et al., 2008). Treatment with 75 nM INCYDE made wild type seedlings fully resistant even to 0.5μM AZD8055 (Fig. 5c + Fig. S11+S15), demonstrating that the enhanced activity of multiple CKX enzymes is likely responsible for mediating the effect of TOR kinase on shoot development and growth. Importantly, contrasting the effect of general inhibition with those of mutations in single genes revealed that individual CKX appeared to differ in their relative contributions, which fitted well with their highly specific expression patterns. The CKX inhibitor dose-response curve also demonstrated that reduction of overall CKX activity did not render seedlings resistant to full block of TOR kinase activity, similar to our results from single *ckx* mutants. This may either be due to incomplete block of CKX enzymes by INCYDE, or explained by a state of cellular dormancy or arrest caused by full block of TOR function, which cannot be rescued by enhancing CK levels.

While fresh weight represented an easily quantifiable proxy for shoot development and growth, it did not allow us to draw any conclusions about the effect of CKX enzymes on *WUS* activity. Since *WUS* RNA levels in seedlings cannot be quantified reliably by other means, we used CRISPR alleles of *CKX5* and *CKX6* in the *WUS* reporter background (Pfeiffer et al., 2016) to investigate SAM specific *WUS* expression in response to TOR.

Supporting our findings at the level of shoot growth, we found that inactivation of *CKX5*, or *CKX5* together with *CKX6* restored *WUS* expression to wild type levels after TOR inhibition, whereas mutation of *CKX6* alone had no effect (Fig. 5b). The untreated *ckx5,6* double mutant exhibited higher basal expression levels of the *WUS* reporter, which were reduced upon AZD8055 treatment but not below wild type mock levels, demonstrating additive genetic interaction between *ckx5* and *ckx6* upstream of *WUS* expression. Again, as for shoot growth, general pharmacological inhibition of CKX activity using INCYDE (Zatloukal et al., 2008) also

rescued *WUS* expression to mock levels in the presence of 2 μM AZD8055 (Fig. 5d). Taken together, these observations demonstrated that active TOR reduced overall CKX gene function allowing CK accumulation, which in turn stimulates *WUS* expression and shoot growth.

TOR inhibition leads to CKX1 protein accumulation

TOR could affect CKX enzymes at various levels from expression of the corresponding genes, to *CKX* mRNA translation, to enzyme activity, or CKX protein stability. Mining our transcriptome data, we found no evidence for significant differential regulation of *CKX* transcripts and RT-qPCR showed a mild but significant increase in transcript abundance for *CKX6*, whereas *CKX2* and *CKX5* transcripts were decreased (Fig. S16). Hence, we concluded that the nature of the molecular interaction between TOR and CKXs likely occurs downstream of the mRNA level.

To distinguish between increased protein accumulation and CKX enzyme activity, we analyzed protein abundance in response to AZD8055. Since there are currently no antibodies against any of the CKX enzymes available, we made use of a *p35S:cMyc-CKX1* translational fusion line (Niemann et al., 2015, 2018). Western blot analysis revealed that eight hours after transfer to AZD8055 containing medium, shoots accumulated 39 – 109 % more cMyc-CKX1 than mock treated shoots in three independent experiments (Fig. 6a). In contrast, AZD8055 did not induce significant changes in *CKX1* transcript abundance in the same experiment (Fig. 6b).

Protein accumulation is either the result of decreased protein turnover or increased protein biosynthesis and hence we first tested if CKX protein stability was affected by TOR inhibition. To this end, we utilized cycloheximide (CHX) to inhibit translational elongation and assayed cMyc-CKX1 protein levels over the course of eight hours with- or without preincubation on AZD8055 for eight hours (Fig. 6c). We found that cMyc-CKX1 turnover rate was very similar in AZD8055 and mock treated shoots and half-life was determined at ~4 h for both, which was in agreement with published results (Niemann et al., 2015). As a result, we concluded that TOR inhibition is unlikely to affect CKX1 protein stability but may rather enhance CKX1 translation to cause the observed protein over-accumulation (Fig. 6a).

TOR controls translation of specific *CKX* transcripts

To test whether TOR controls translation of CKX transcripts, we applied polysome profiling and quantified the association of different *CKX* mRNAs with highly translating polysomes in mock and AZD8055 treated shoots (Fig. 7 + Fig. S17 + S18). Consistent with the enhanced

protein accumulation of CKX1, we observed a strong enrichment of *CKX1* mRNA in the heavy polysome fractions (fractions 1-3) of AZD8055 treated samples, which suggested that more CKX1 protein was synthesized at the ribosomes after eight hours of TOR inhibition compared to mock treated controls. Similarly, we observed accumulation of *CKX5* and *CKX3* transcripts in polysomal fractions from inhibitor treated seedlings (Fig. 7), which fitted well with the observed resistance of the *ckx5* and *ckx3* mutants towards AZD8055 (Fig. 5a+b+e+f). Due to its low expression levels we could detect *CKX3* transcripts only in one of three replicates tested. *CKX6* and *CKX7* transcripts were overall similar in treated and mock samples with a moderate increase in some of the lighter polysomal fractions (fractions 3-5) following AZD8055 treatment (Fig. 7 + S18). The lower enrichment of *CKX6* mRNAs in polysomes compared to *CKX5* fitted well with the behavior in our physiological assays observed for the respective mutants (Fig. 5a + Fig. 5b). *CKX4* transcripts did not differ significantly between mock and treatment due to large experimental variations between replicates (Fig. 7 + Fig S18). In conclusion, our experiments showed that translation of multiple transcripts encoding CKX enzymes was controlled by TOR activity. In particular CKX1, CKX3 and CKX5 protein biosynthesis appeared to be repressed when TOR is active, which fitted well with functional data on CKX5 and CKX3 (Fig. 5) and with protein analysis of CKX1 (Fig. 6). Our data on *CKX4* did not allow us to draw solid conclusions on translational control (Fig. 7 + Fig S18), however our genetic data showed a clear antagonistic effect between TOR and CKX4, which was in line with a trend towards accumulation in heavy polysomes after treatment (Fig. 5e+f + Fig. S14). Close inspection of the 5´-leader sequences of all *CKX* encoding genes revealed that only *CKX4* contains a strong uORF signature that may have influenced the observed response to TOR inhibition.

In sum, our results demonstrated that TOR kinase controls *WUS* expression and partially shoot development via regulation of cytokinin levels, specifically *tZ*. This effect is mediated through modulation of protein accumulation of specific CKX cytokinin degrading enzymes. Mechanistically, TOR controls transcription of several CK pathway genes, and restricts CKX protein accumulation by repressing *CKX* mRNA translation.

Discussion

Plants dynamically adjust their transcriptional and translational programs to quickly adapt to changing environments. The TOR kinase network is a master regulator of cellular metabolism and controls translation in accordance with nutrient availability in all eukaryotes. Several reports have shown a connection between TOR and stem cell activity in plants and identified upstream regulators for this specific function in diverse settings (Li et al., 2017; Pfeiffer et al.,

2016; Xiong et al., 2013). However, the downstream effectors connecting TOR with stem cell regulatory programs so far remained elusive. Focusing on shoot stem cells, we show that TOR controls accumulation of specific CK species by translational repression of individual CKX transcripts (Fig. 6a, Fig. 7 + S18). CKX enzyme activity in turn limits the availability of *trans*-zeatin, the major instructive signal for SAM development and *WUS* expression (Fig. 3+4+5b+c).

CKX enzymes catalyze the irreversible degradation of CKs and hence exert strong influence on development and growth (Bartrina et al., 2011). Cytokinins are potent regulators of plant growth and development and act as long-distance signaling molecules that instruct cellular identity and behavior of diverse tissues, including the SAM (Kieber & Schaller, 2014; Landrein et al., 2018; Osugi et al., 2017). Thus, controlling CK abundance is key to synchronizing SAM activity with cellular homeostasis of distant source tissues that take up or produce the resources necessary for organogenesis and growth. Our results suggest that TOR under favorable conditions represses translation of CKX mRNAs, whereas when TOR is inhibited, CKX translational efficiency is enhanced resulting in globally reduced levels of *trans*-zeatin and ultimately in reduced activity of stem cells in the SAM. This active translational repression enables global adjustments of CK availability faster compared with transcriptional adjustments and might therefore grant a fitness advantage. Importantly, we found that CKX enzymes mediate control of plant growth only when TOR is at least partially active, since at higher concentrations of AZD8055 inhibitor, we did not observe any epistasis. This may suggest that CK only governs part of TOR mediated growth control, or that the cellular response to strong inhibition of TOR does not allow growth because of cellular dormancy.

Intriguingly, not all CK metabolites appear equally affected by TOR inhibition as *i*P levels are increased, whereas *i*PRMP and most *tZ* metabolites are reduced. Similarly, CK response towards exogenously added *tZ* is impaired, while response towards *i*P is not, both suggesting differential degradation of specific CK species. One explanation could be different selectivity profiles of CKX enzymes towards certain CK species and indeed, several CKX enzymes show a higher affinity towards *tZ* compared with *i*P bases in *in vitro* activity assays (Galuszka et al., 2007; Kowalska et al., 2010). Interestingly, especially CKX1, which showed the clearest response to TOR inhibition in our polysome profiles, strongly prefers *tZ*. *In vivo* evidence comes from the characterization of *ckx3 ckx5* double mutants (Bartrina et al., 2011) that show accumulation of *tZ* but have unaltered *i*P levels and whose *tZ* and *i*P profiles are inverse to the ones from AZD8055 treated plants presented in this study. Together with our observation that *CKX3* and *CKX5* mRNAs accumulated in polysomal fractions and that the respective

single mutants showed resistance towards TOR inhibition, this strongly supports the notion that CKX activity is the major driver of TOR dependent changes of CK metabolites.

Our results did not allow us to draw conclusions about the detailed molecular mechanism by which TOR activity results in translational repression of specific transcripts. However, one potential mechanism might involve SnRK1 dependent translation mediated by eIFiso4G, although translational efficiency data of eIFiso4G mutants show no evidence for differential translation of CKX transcripts (Cho et al., 2019). Alternatively, GCN2 dependent translation via eiF2alpha could drive translation antagonistically to TOR (Y. Dong et al., 2017; Sesma et al., 2017).

Our polysome data showed differential responses of CKX mRNAs to TOR inhibition in seedling shoots, raising the question of regulatory specificity. While individual CKX transcripts exhibit structural differences that may underly their specific responses to TOR dependent translational repression, differential regulatory effects may also arise from divergent cellular contexts. CKX transcripts have highly specific expression patterns (Bartrina et al., 2011; Werner et al., 2003) and thus some of the differences we have observed may therefore be caused by differential cellular response to TOR inhibition, for example in source versus sink tissues. Along these lines, differences in TOR activity between source and sink tissues resulting in inverse regulation of plasmodesmata permeability have recently been demonstrated (Brunkard et al., 2020). These cell type specific function could not only be responsible for the differences between specific CKX transcripts, but also underly the diversity in responses we observed for some CKX genes across diverse experiments. In particular, the divergent behavior of *ckx5*, *ckx6,* and *ckx5/6* mutants in growth, *WUS* reporter and polysome assays is worth mentioning. First, *ckx6* single mutant seedlings showed some resistance to AZD8055 in our shoot growth assay even though we observed no major differences on the polysome level. However, *CKX6* was the only transcript that showed enhanced accumulation in qRT-PCR after TOR inhibition which could explain how *CKX6* is linked to TOR. Importantly, in *ckx6* mutant seedlings WUS expression after TOR inhibition was indistinguishable from wild type, which could be due to specific *CKX6* expression patterns restricting its effect to distinct CK dependent traits. Second, the genetic interaction of *CKX5 and CKX6* was complex: Both single mutants were resistant to TOR inhibition in shoot growth assays, however only *ckx5* had an effect in the *WUS* reporter assay. Interestingly, *ckx5/6* double mutants showed an positive genetic interaction in the *WUS* reporter assay, whereas for shoot growth it was negative with the *ckx5/6* double mutants showing less resistance than any of the single mutants. Again, tissue specific CKX expression patterns that change in response to loss of function of other CKX genes together with tissue specific responses to TOR activity could

underly this complex behavior. While previous studies showed a correlation between *tZ* abundance, *WUS* expression and shoot growth, our data reveal that *WUS* expression and thus stem cell activity are only one element in a complex regulatory network. It remains to be deciphered if this complexity arises at the level of tissue specific TOR activities, or rather at the level of differential CK responses. In any case, by controlling CK homeostasis, or through other mechanisms TOR does influence a large number of growth-related processes such as cellular expansion, proliferation and cellular homeostasis indicated by several thousand genes we identified initially.

Interfering with CK homeostasis through targeted expression of CKXs can increase plants resilience to environmental stresses such as drought or cold and improve yield traits (Ashikari et al., 2005; Cortleven et al., 2019; Nehnevajova et al., 2019; Schwarz et al., 2020) and thus represent promising candidates of agronomic importance (Jameson & Song, 2020). Consequently, misexpression of CKXs has been successfully employed to generate improved crops and targeted translational control bears the potential to generate cultivars that ameliorate the detrimental effects of broad CKX overexpression. Along these lines, we observed that the supplementation of sugars together with CKs is sufficient to drive *WUS* expression even when TOR is inactive. This further fuels the question about specific TOR functions in stem cells compared to differentiated tissues, since in this context CKs are not necessarily degraded in the SAM, although some CKX isoforms are specifically expressed in the OC (Bartrina et al., 2011; Werner et al., 2003).

Taken together, our findings on TOR mediated translational repression of catabolic enzymes open new avenues to study the mechanisms of TOR driven environmental adaptation and stem cell control. Considering the ecological benefits that could conceptually be derived from tunable translational repression of growth factor catabolism, this regulatory logic may be much more widespread than anticipated so far.

Materials and methods

Plant material

All used plant lines were in the Col-0 background. The double reporter line pWUS:3xVenus:NLS/ pCLV3:mCherry:NLS as well as the *ckx5*, *ckx6* and *ckx5/ckx6* CRISPR mutants were described in (Pfeiffer et al., 2016). The p35S:ARR1ΔDDK:GR line was described in (Sakai et al., 2001a) and was crossed with the double reporter line to obtain homozygous alleles for each transgene. The p35S:cMyc-CKX1 line was described in (Niemann et al., 2015, 2018). The ckx2 (SALK_083761c), ckx3 (SALK_050938c), ckx4 (SALK_055204c) mutants were obtained from NASC. The *cre1-2/ahk3-7* mutant was described in (Riefler et al., 2006).

Growth conditions

Seeds were sterilized with 70% ethanol and 0.1% Triton for 10 min and afterwards washed twice with autoclaved water. Seeds were plated on 100 μm nylon meshes (nitex 03/100–44, Sefar, Heiden, Switzerland) on top of 0.5x MS (Duchefa, Haarlem, The Netherlands), 0.9% Phytoagar in square petri dishes. After plating, seeds were imbibed for 3 days at 4°C in darkness and transferred to growth cabinets (poly klima, PK 520-LED, Freising, Germany) where they were kept under continuous light at 22°C and grown vertically for 4 days. Subsequently, seedlings were transferred with the nylon meshes to 0.5x MS plates supplemented with 2 μM AZD8055 (Selleckchem, Houston, TX) or equal volumes of DMSO for 8 h.

Liquid culture

About 30–40 seeds imbibed as described above, were sown in 3 ml 0.5x MS in petri dishes of 35 mm diameter. Plants were kept in darkness for three days after the induction of germination by 6 hr light treatment. The medium of two day old etiolated seedlings was supplemented with the indicated treatments. All stock solutions were 1000x concentrated and diluted in DMSO, therefore control plants were mock treated with the same volume of DMSO.

RNAseq

Seedlings were grown as described under growth conditions. 4 days after germination seedlings were transferred on a mesh to 0.5xMS plates containing either 2 μM AZD8055, 10 μM TORIN1, 20 μM KU63794 or equal volumes of DMSO as mock control. After 8 h, 30 mg of shoot tissue were harvested for each replicate and frozen in liquid nitrogen. 3 independent

replicates were harvested for each condition. Total RNA was extracted with the Plant RNA Purification Reagent (Invitrogen, Carlsbad, CA) according to the instructions of the manufacturer, digested with TURBO DNAse (Ambion/ Thermo Fisher, Waltham, MA) and purified with RNeasy Mini Kit (Quiagen, Hilden, Germany). Libraries were poly-(A) selected and analyzed with NEXTseq 500. For differential gene expression analysis reads were aligned with RNA STAR (v2.6) alignment tool with TAIR10 genome model as reference. Transcripts were assembled and counted with StringTie (v1.3.3) and statistical analysis was performed using DESeq2 (v1.18.1) (Love et al., 2014). GO term analysis was performed using ThaleMine web tool (https://www.bar.utoronto.ca/thalemine/begin.do).

Histochemical GUS staining

Four day old seedlings were harvested in 90% acetone and incubated at –20°C for at least 1 hr. Seedlings were washed with PBS and incubated in substrate buffer (1x PBS (pH 7.0), 1 mM $K_3Fe(III)(CN)_6$, 0.5 mM $K_4Fe(II)(CN)_6$, 1 mM EDTA, 1% Triton X-100, 1 mg/ml X-gluc) at 22°C over night. After staining, the seedlings were incubated with 60% and subsequently in 95% ethanol to remove chlorophyll.

Microscopy and fluorescence quantification

All images were obtained using Zeiss Imager M1, the Plan-APOCHROMAT 20x/0.8 objective (Zeiss, Oberkochen, Germany) and YFP- and GFP-specific filter sets. Procedures for fluorescent reporter activities of the double reporter were performed as described in (Pfeiffer et al., 2016). Each measurement was normalized to the median (set to 100) of the mock for experiments in the light or to the 6-BA treated samples for experiments performed in the dark.

Western blot

Approximately 30 mg of shoot tissue were harvested, and proteins were extracted with 1:4 ratio (mg/μl) adjusted to the exact fresh weight with 95°C hot denaturing buffer (100 mM MOPS pH 7.6, 100 mM NaCl, 40 mM ß-MeOH, 5% SDS, 10% Glycerol, 4 mM EDTA, 2 mM PMSF, PI (Sigma)) and boiled at 95°C for 5 min. Cellular debris was removed by two centrifugation steps (10 min, 14,000 rpm, RT). Equal volumes of the obtained extract were separated on a 10% SDS-PAGE gel and blotted to a PVDF membrane. Membranes were probed with Phospho-p70 S6 kinase (Thr(P)-389) polyclonal antibody (No.9205, Cell Signaling Technology, Cambridge, UK) to detect S6K phosphorylation. S6K1/2 antibody (AS12-1855, Agrisera AB, Vännäs, Sweden) was used to detect total S6K1 and S6K2. c-Myc antibody (9E10, Santa Cruz Biotechnology, Dallas, TX) was used to detect c-Myc tagged CKX1.

Physiology

Seeds were singled out on 0.5xMS, 0.9% Phytoagar plates and imbibed for three days at 4°C in the dark. Plates were kept horizontally in long day conditions at 22°C for four days. ~ 40 single seedlings at the same developmental stage and of similar size were selected and transferred to plates containing the indicated AZD8055 concentrations and grown for seven more days before shoot fresh weight was measured. For the measurements, seedling shoots were removed and weighed in batches of 5 – 10 seedlings. Afterwards the average weight was calculated for each batch.

Statistical testing

Statistical analysis for experiments shown in Fig. 5a+e, linear mixed models were ("lme4" package "R") were generated with Genotype (Freshweight ~ AZDconcentration*Genotype + (1|Experiment)) or without Genotype (Freshweight ~ AZDconcentration + (1|Experiment)) and compared with ANOVA to calculate the p-value for significant interaction. For Fig. 5c a linear model with (Freshweight ~ AZDconcentration*Treatment) was compared with (Freshweight ~ AZDconcentration) using ANOVA. Datasets were previously evaluated for extreme outliers, normality assumptions and heteroscedasticity. Pairwise t-tests have been performed for group comparisons with Bonferroni correction. Statistical analysis was performed in R (v4.0.2) with unnormalized data. ED50 values were calculated using the "drc" package for dose response analysis in R (Ritz et al., 2015). The dose of effect ratios in Fig. 5f were calculated with the *EDcomp* function from the "drc" package with the *delta* method to estimate confidence intervals. To test if ED50 values are significantly different dose response models for each mutant line and the wild type were generated and compared with a model that assumes the curves are the same using ANOVA as described in (Ritz et al., 2015).

Data that was not normally distributed was tested with Wilcoxon rank test and Hochberg correction. Normally distributed data was tested for heteroscedasticity and two-tailed students t-test with equal or unequal variance have been performed accordingly.

CHX chase assay

P35S:cMyc-CKX1 seedlings were grown as described under growth conditions. 8 h after transfer to 2 μM AZD8055 the plates were flooded with 50 ml 200 μM cycloheximide and 2μM AZD8055 solution (0.015% Silwet L-77) for 0, 2, 4 and 8 h and shoots were harvested for western blot analysis as described above.

RT-qPCR

Total RNA was extracted as described under RNAseq. RNA integrity was confirmed on an agarose gel and the concentrations were determined with a nanodrop device. Equal amounts of RNA were used for oligo dT primed cDNA synthesis with the RevertAid First Strand cDNA Synthesis Kit (Thermo Fisher, Waltham, MA). The qPCR reaction was set up using the SG qPCR Master Mix (EURx, Gdansk, Poland) and run on a qTOWER^3 (Analytic Jena, Jena, Germany) PCR System with technical duplicates each.

Cytokinin profiling – LC-MS

For cytokinin profiling seedlings were grown as described for RNAseq analysis and 5 biological replicates of shoot tissue were harvested for each condition. The CK content was determined by ultra-high performance liquid chromatography-electrospray tandem mass spectrometry (Svačinová et al., 2012), including modifications described by (Antoniadi et al., 2015). Briefly, samples (20 mg FW) were homogenized and extracted in 1 ml of modified Bieleski buffer (60% methanol, 10% HCOOH and 30% H_2O) together with a cocktail of stable isotope-labeled internal standards (0.25 pmol of CK bases, ribosides, *N*-glucosides, and 0.5 pmol of CK *O*-glucosides, nucleotides per sample added). The extracts were purified onto an Oasis MCX column (30 mg/1 ml, Waters) and then analyzed using using an Acquity I-class system (Waters, Milford, MA, USA) combined with a mass spectrometer Xevo™ TQ-XS (Waters, Manchester, UK). Data were processed with Target Lynx V4.2 software and final concentration levels of phytohormones were calculated using isotope dilution method (Novák et al., 2008).

Polysome fractionation

200 mg plant material grown as described under growth conditions was homogenized by rotating at 4°C in 600 ul polysome extraction buffer (0.2 mM Tris-HCL, pH=9, 0.2 mM KCL, 25 mM EGTA, 35 mM MgCl2, 1% DOC, 1% PTE, 1% Brij-35, 1% Triton X-100, 1% NP-40, 1% Tween-20, 5 mM DTT, 10 μM MG-132, 50 μg/ml Cycloheximide, 50 μg/ml chloramphenicol and 1% EDTA-free protease inhibitor cocktail). Extracts were centrifuged at 16000xg at 4°C for 10 min. 300 μl supernatant was loaded to 7-47% sucrose gradient and centrifuged at 38000x rpm for 3 hours in a Beckmann SW41Ti rotor. The gradient was fractionated after recording the absorbance at 254 nm. RNA was precipitated from 1 ml fraction by mix and incubation with one volume of 8 M guanidine-HCL and two volumes of absolute ethanol at -20°C over night followed by centrifuge at max. speed for 1 hour. RNA pellet was resuspended with 50 μl DEPC water. 100 ng RNA was used for cDNA synthesis (SuperScript IV reverse

transcriptase (ThermoFisher, 18090050) which was subsequently analysed by qRT-PCR as described above.

Cytokinin response assay

Seedlings were grown as described under growth conditions. After 8 h of AZD8055 or mock treatment seedlings were sprayed with an atomizer with either 100 nM of trans-zeatin (Duchefa, Haarlem, The Netherlands) or 100 nM of isopentyladenine (Duchefa, Haarlem, The Netherlands) solution (0.015% Silwet L-77). After 30 min three independent replicates of shoots and roots were harvested separately for total RNA extraction and RT-qPCR analysis as described above.

References

Antoniadi, I., Novák, O., Gelová, Z., Johnson, A., Plíhal, O., Simerský, R., Mik, V., Vain, T., Mateo-Bonmatí, E., Karady, M., Pernisová, M., Plačková, L., Opassathian, K., Hejátko, J., Robert, S., Friml, J., Doležal, K., Ljung, K., & Turnbull, C. (2020). Cell-surface receptors enable perception of extracellular cytokinins. *Nature Communications*, *11*(1), 4284. https://doi.org/10.1038/s41467-020-17700-9

Antoniadi, I., Plačková, L., Simonovik, B., Doležal, K., Turnbull, C., Ljung, K., & Novák, O. (2015). Cell-type-specific cytokinin distribution within the Arabidopsis primary root apex. *The Plant Cell*, *27*(7), 1955–1967.

Ashikari, M., Sakakibara, H., Lin, S., Yamamoto, T., Takashi, T., Nishimura, A., Angeles, E. R., Qian, Q., Kitano, H., & Matsuoka, M. (2005). Cytokinin Oxidase Regulates Rice Grain Production. *Science*, *309*(5735), 741–745. https://doi.org/10.1126/science.1113373

Bartrina, I., Otto, E., Strnad, M., Werner, T., & Schmülling, T. (2011). Cytokinin regulates the activity of reproductive meristems, flower organ size, ovule formation, and thus seed yield in Arabidopsis thaliana. *The Plant Cell*, *23*(1), 69–80.

Bäurle, I., & Laux, T. (2005). Regulation of WUSCHEL transcription in the stem cell niche of the Arabidopsis shoot meristem. *The Plant Cell*, *17*(8), 2271–2280.

Brunkard, J. O., Xu, M., Scarpin, M. R., Chatterjee, S., Shemyakina, E. A., Goodman, H. M., & Zambryski, P. (2020). TOR dynamically regulates plant cell–cell transport. *Proceedings of the National Academy of Sciences*, *117*(9), 5049–5058. https://doi.org/10.1073/pnas.1919196117

Buechel, S., Leibfried, A., To, J. P. C., Zhao, Z., Andersen, S. U., Kieber, J. J., & Lohmann, J. U. (2010). Role of A-type ARABIDOPSIS RESPONSE REGULATORS in meristem maintenance and regeneration. *European Journal of Cell Biology*, *89*(2), 279–284. https://doi.org/10.1016/j.ejcb.2009.11.016

Caldana, C., Li, Y., Leisse, A., Zhang, Y., Bartholomaeus, L., Fernie, A. R., Willmitzer, L., & Giavalisco, P. (2013). Systemic analysis of inducible target of rapamycin mutants reveal a general metabolic switch controlling growth in Arabidopsis thaliana. *The Plant Journal*, *73*(6), 897–909. https://doi.org/10.1111/tpj.12080

Cho, H.-Y., Lu, M.-Y. J., & Shih, M.-C. (2019). The SnRK1-eIFiso4G1 signaling relay regulates the translation of specific mRNAs in Arabidopsis under submergence. *New Phytologist*, *222*(1), 366–381. https://doi.org/10.1111/nph.15589

Cortleven, A., Leuendorf, J. E., Frank, M., Pezzetta, D., Bolt, S., & Schmülling, T. (2019). Cytokinin action in response to abiotic and biotic stresses in plants. *Plant, Cell & Environment*, *42*(3), 998–1018. https://doi.org/10.1111/pce.13494

Dai, X., Liu, Z., Qiao, M., Li, J., Li, S., & Xiang, F. (2017). *ARR12 promotes de novo shoot regeneration in Arabidopsis thaliana via activation of WUSCHEL expression*. *59*(10), 12.

Daum, G., Medzihradszky, A., Suzaki, T., & Lohmann, J. U. (2014). A mechanistic framework for noncell autonomous stem cell induction in Arabidopsis. *Proceedings of the National Academy of Sciences*, *111*(40), 14619–14624.

Dobrenel, T., Caldana, C., Hanson, J., Robaglia, C., Vincentz, M., Veit, B., & Meyer, C. (2016). TOR Signaling and Nutrient Sensing. *Annual Review of Plant Biology*, *67*(1), 261–285. https://doi.org/10.1146/annurev-arplant-043014-114648

Dong, P., Xiong, F., Que, Y., Wang, K., Yu, L., Li, Z., & Maozhi, R. (2015). Expression profiling and functional analysis reveals that TOR is a key player in regulating photosynthesis and phytohormone signaling pathways in Arabidopsis. *Frontiers in Plant Science*, *6*, 677. https://doi.org/10.3389/fpls.2015.00677

Dong, Y., Silbermann, M., Speiser, A., Forieri, I., Linster, E., Poschet, G., Allboje Samami, A., Wanatabe, M., Sticht, C., Teleman, A. A., Deragon, J.-M., Saito, K., Hell, R., &

Wirtz, M. (2017). Sulfur availability regulates plant growth via glucose-TOR signaling. *Nature Communications*, *8*(1), 1174. https://doi.org/10.1038/s41467-017-01224-w

Fu, L., Liu, Y., Qin, G., Wu, P., Zi, H., Xu, Z., Zhao, X., Wang, Y., Li, Y., Yang, S., Peng, C., Wong, C. C. L., Yoo, S.-D., Zuo, Z., Liu, R., Cho, Y.-H., & Xiong, Y. (2021). The TOR–EIN2 axis mediates nuclear signalling to modulate plant growth. *Nature*, *591*(7849), 288–292. https://doi.org/10.1038/s41586-021-03310-y

Gajdošová, S., Spíchal, L., Kamínek, M., Hoyerová, K., Novák, O., Dobrev, P. I., Galuszka, P., Klíma, P., Gaudinová, A., Žižková, E., Hanuš, J., Dančák, M., Trávníček, B., Pešek, B., Krupička, M., Vaňková, R., Strnad, M., & Motyka, V. (2011). Distribution, biological activities, metabolism, and the conceivable function of cis-zeatin-type cytokinins in plants. *Journal of Experimental Botany*, *62*(8), 2827–2840. https://doi.org/10.1093/jxb/erq457

Galuszka, P., Popelková, H., Werner, T., Frébortová, J., Pospíšilová, H., Mik, V., Köllmer, I., Schmülling, T., & Frébort, I. (2007). Biochemical characterization of cytokinin oxidases/dehydrogenases from Arabidopsis thaliana expressed in Nicotiana tabacum L. *Journal of Plant Growth Regulation*, *26*(3), 255–267.

Gordon, S. P., Chickarmane, V. S., Ohno, C., & Meyerowitz, E. M. (2009). Multiple feedback loops through cytokinin signaling control stem cell number within the Arabidopsis shoot meristem. *Proceedings of the National Academy of Sciences*, *106*(38), 16529–16534. https://doi.org/10.1073/pnas.0908122106

Gruel, J., Landrein, B., Tarr, P., Schuster, C., Refahi, Y., Sampathkumar, A., Hamant, O., Meyerowitz, E. M., & Jönsson, H. (2016). An epidermis-driven mechanism positions and scales stem cell niches in plants. *Science Advances*, *2*(1), e1500989. https://doi.org/10.1126/sciadv.1500989

Heyl, A., Werner, T., & Schmülling, T. (2018). Cytokinin Metabolism and Signal Transduction. In J. A. Roberts (Ed.), *Annual Plant Reviews online* (pp. 93–123). John Wiley & Sons, Ltd. https://doi.org/10.1002/9781119312994.apr0245

Hluska, T., Šebela, M., Lenobel, R., Frébort, I., & Galuszka, P. (2017). Purification of Maize Nucleotide Pyrophosphatase/Phosphodiesterase Casts Doubt on the Existence of Zeatin Cis–Trans Isomerase in Plants. *Frontiers in Plant Science*, *8*, 1473. https://doi.org/10.3389/fpls.2017.01473

Holst, K., Schmülling, T., & Werner, T. (2011). Enhanced cytokinin degradation in leaf primordia of transgenic Arabidopsis plants reduces leaf size and shoot organ primordia formation. *Journal of Plant Physiology*, *168*(12), 1328–1334.

Jameson, P. E., & Song, J. (2020). Will cytokinins underpin the second 'Green Revolution'? *Journal of Experimental Botany*, *71*(22), 6872–6875. https://doi.org/10.1093/jxb/eraa447

Janocha, D., & Lohmann, J. U. (2018). From signals to stem cells and back again. *Current Opinion in Plant Biology*, *45*, 136–142. https://doi.org/10.1016/j.pbi.2018.06.005

Kasahara, H., Takei, K., Ueda, N., Hishiyama, S., Yamaya, T., Kamiya, Y., Yamaguchi, S., & Sakakibara, H. (2004). Distinct Isoprenoid Origins of cis- and trans-Zeatin Biosyntheses in Arabidopsis. *Journal of Biological Chemistry*, *279*(14), 14049–14054. https://doi.org/10.1074/jbc.M314195200

Kiba, T., Takei, K., Kojima, M., & Sakakibara, H. (2013). Side-Chain Modification of Cytokinins Controls Shoot Growth in Arabidopsis. *Developmental Cell*, *27*(4), 452–461. https://doi.org/10.1016/j.devcel.2013.10.004

Kieber, J. J., & Schaller, G. E. (2014). Cytokinins. *The Arabidopsis Book / American Society of Plant Biologists*, *12*. https://doi.org/10.1199/tab.0168

Köllmer, I., Novák, O., Strnad, M., Schmülling, T., & Werner, T. (2014). Overexpression of the cytosolic cytokinin oxidase/dehydrogenase (CKX 7) from A rabidopsis causes

specific changes in root growth and xylem differentiation. *The Plant Journal*, *78*(3), 359–371.

Kowalska, M., Galuszka, P., Frébortová, J., Šebela, M., Béres, T., Hluska, T., Šmehilová, M., Bilyeu, K. D., & Frébort, I. (2010). Vacuolar and cytosolic cytokinin dehydrogenases of Arabidopsis thaliana: Heterologous expression, purification and properties. *Phytochemistry*, *71*(17–18), 1970–1978. https://doi.org/10.1016/j.phytochem.2010.08.013

Kuroha, T., Tokunaga, H., Kojima, M., Ueda, N., Ishida, T., Nagawa, S., Fukuda, H., Sugimoto, K., & Sakakibara, H. (2009). Functional Analyses of LONELY GUY Cytokinin-Activating Enzymes Reveal the Importance of the Direct Activation Pathway in Arabidopsis. *The Plant Cell*, *21*(10), 3152–3169. https://doi.org/10.1105/tpc.109.068676

Landrein, B., Formosa-Jordan, P., Malivert, A., Schuster, C., Melnyk, C. W., Yang, W., Turnbull, C., Meyerowitz, E. M., Locke, J. C. W., & Jönsson, H. (2018). Nitrate modulates stem cell dynamics in *Arabidopsis* shoot meristems through cytokinins. *Proceedings of the National Academy of Sciences*, *115*(6), 1382–1387. https://doi.org/10.1073/pnas.1718670115

Laux, T., Mayer, K. F. X., Berger, J., & Jürgens, G. (1996). *The WUSCHEL gene is required for shoot and floral meristem integrity in Arabidopsis*. 10.

Li, X., Cai, W., Liu, Y., Li, H., Fu, L., Liu, Z., Xu, L., Liu, H., Xu, T., & Xiong, Y. (2017). Differential TOR activation and cell proliferation in *Arabidopsis* root and shoot apexes. *Proceedings of the National Academy of Sciences*, *114*(10), 2765–2770. https://doi.org/10.1073/pnas.1618782114

Liu, G. Y., & Sabatini, D. M. (2020). MTOR at the nexus of nutrition, growth, ageing and disease. *Nature Reviews Molecular Cell Biology*, *21*(4), 183–203. https://doi.org/10.1038/s41580-019-0199-y

Liu, Q., Kirubakaran, S., Hur, W., Niepel, M., Westover, K., Thoreen, C. C., Wang, J., Ni, J., Patricelli, M. P., Vogel, K., Riddle, S., Waller, D. L., Traynor, R., Sanda, T., Zhao, Z., Kang, S. A., Zhao, J., Look, A. T., Sorger, P. K., … Gray, N. S. (2012). Kinome-wide Selectivity Profiling of ATP-competitive Mammalian Target of Rapamycin (mTOR) Inhibitors and Characterization of Their Binding Kinetics*,. *Journal of Biological Chemistry*, *287*(13), 9742–9752. https://doi.org/10.1074/jbc.M111.304485

Love, M. I., Huber, W., & Anders, S. (2014). Moderated estimation of fold change and dispersion for RNA-seq data with DESeq2. *Genome Biology*, *15*(12), 550. https://doi.org/10.1186/s13059-014-0550-8

Malinovsky, F. G., Thomsen, M.-L. F., Nintemann, S. J., Jagd, L. M., Bourgine, B., Burow, M., & Kliebenstein, D. J. (2017). An evolutionarily young defense metabolite influences the root growth of plants via the ancient TOR signaling pathway. *ELife*, *6*, e29353. https://doi.org/10.7554/eLife.29353

Mayer, K. F. X., Schoof, H., Haecker, A., Lenhard, M., Jürgens, G., & Laux, T. (1998). Role of WUSCHEL in Regulating Stem Cell Fate in the Arabidopsis Shoot Meristem. *Cell*, *95*(6), 805–815. https://doi.org/10.1016/S0092-8674(00)81703-1

Menand, B., Desnos, T., Nussaume, L., Berger, F., Bouchez, D., Meyer, C., & Robaglia, C. (2002). Expression and disruption of the Arabidopsis TOR (target of rapamycin) gene. *Proceedings of the National Academy of Sciences*, *99*(9), 6422–6427. https://doi.org/10.1073/pnas.092141899

Meng, W. J., Cheng, Z. J., Sang, Y. L., Zhang, M. M., Rong, X. F., Wang, Z. W., Tang, Y. Y., & Zhang, X. S. (2017). Type-B ARABIDOPSIS RESPONSE REGULATORs Specify the Shoot Stem Cell Niche by Dual Regulation of *WUSCHEL*. *The Plant Cell*, *29*(6), 1357–1372. https://doi.org/10.1105/tpc.16.00640

Miyawaki, K., Tarkowski, P., Matsumoto-Kitano, M., Kato, T., Sato, S., Tarkowska, D., Tabata, S., Sandberg, G., & Kakimoto, T. (2006). Roles of Arabidopsis ATP/ADP

isopentenyltransferases and tRNA isopentenyltransferases in cytokinin biosynthesis. *Proceedings of the National Academy of Sciences*, *103*(44), 16598–16603. https://doi.org/10.1073/pnas.0603522103

Montané, M.-H., & Menand, B. (2019). TOR inhibitors: From mammalian outcomes to pharmacogenetics in plants and algae. *Journal of Experimental Botany*, *70*(8), 2297–2312. https://doi.org/10.1093/jxb/erz053

Nehnevajova, E., Ramireddy, E., Stolz, A., Gerdemann-Knörck, M., Novák, O., Strnad, M., & Schmülling, T. (2019). Root enhancement in cytokinin-deficient oilseed rape causes leaf mineral enrichment, increases the chlorophyll concentration under nutrient limitation and enhances the phytoremediation capacity. *BMC Plant Biology*, *19*(1), 83. https://doi.org/10.1186/s12870-019-1657-6

Niemann, M. C. E., Bartrina, I., Ashikov, A., Weber, H., Strnad, M., Strasser, R., Bakker, H., & Schmülling, T. (2015). Arabidopsis ROCK1 transports UDP-GlcNAc/UDP- GalNAc and regulates ER protein quality control and cytokinin activity. *PLANT BIOLOGY*, 6.

Niemann, M. C. E., Weber, H., Hluska, T., Leonte, G., Anderson, S. M., Novák, O., Senes, A., & Werner, T. (2018). The Cytokinin Oxidase/Dehydrogenase CKX1 Is a Membrane-Bound Protein Requiring Homooligomerization in the Endoplasmic Reticulum for Its Cellular Activity. *Plant Physiology*, *176*(3), 2024–2039. https://doi.org/10.1104/pp.17.00925

Novák, O., Hauserová, E., Amakorová, P., Doležal, K., & Strnad, M. (2008). Cytokinin profiling in plant tissues using ultra-performance liquid chromatography–electrospray tandem mass spectrometry. *Phytochemistry*, *69*(11), 2214–2224. https://doi.org/10.1016/j.phytochem.2008.04.022

Osugi, A., Kojima, M., Takebayashi, Y., Ueda, N., Kiba, T., & Sakakibara, H. (2017). Systemic transport of trans-zeatin and its precursor have differing roles in

Arabidopsis shoots. *Nature Plants*, *3*(8), 17112. https://doi.org/10.1038/nplants.2017.112

Pfeiffer, A., Janocha, D., Dong, Y., Medzihradszky, A., Schöne, S., Daum, G., Suzaki, T., Forner, J., Langenecker, T., Rempel, E., Schmid, M., Wirtz, M., Hell, R., & Lohmann, J. U. (2016). Integration of light and metabolic signals for stem cell activation at the shoot apical meristem. *ELife*, *5*, e17023. https://doi.org/10.7554/eLife.17023

Pu, Y., Luo, X., & Bassham, D. C. (2017). TOR-Dependent and -Independent Pathways Regulate Autophagy in Arabidopsis thaliana. *Frontiers in Plant Science*, *8*, 1204. https://doi.org/10.3389/fpls.2017.01204

Ren, M. (2015). TOR-inhibitor insensitive-1 (TRIN1) regulates cotyledons greening in Arabidopsis. *Frontiers in Plant Science*, *6*, 13.

Riefler, M., Novak, O., Strnad, M., & Schmülling, T. (2006). Arabidopsis Cytokinin Receptor Mutants Reveal Functions in Shoot Growth, Leaf Senescence, Seed Size, Germination, Root Development, and Cytokinin Metabolism. *The Plant Cell*, *18*(1), 40–54. https://doi.org/10.1105/tpc.105.037796

Ritz, C., Baty, F., Streibig, J. C., & Gerhard, D. (2015). Dose-Response Analysis Using R. *PLOS ONE*, *10*(12), e0146021. https://doi.org/10.1371/journal.pone.0146021

Romanov, G. A., Lomin, S. N., & Schmülling, T. (2006). Biochemical characteristics and ligand-binding properties of Arabidopsis cytokinin receptor AHK3 compared to CRE1/AHK4 as revealed by a direct binding assay. *Journal of Experimental Botany*, *57*(15), 4051–4058. https://doi.org/10.1093/jxb/erl179

Sakai, H., Honma, T., Aoyama, T., Sato, S., Kato, T., Tabata, S., & Oka, A. (2001b). ARR1, a Transcription Factor for Genes Immediately Responsive to Cytokinins. *Science*, *294*(5546), 1519–1521. https://doi.org/10.1126/science.1065201

Scarpin, M. R., Leiboff, S., & Brunkard, J. O. (2020). Parallel global profiling of plant TOR dynamics reveals a conserved role for LARP1 in translation. *ELife*, *9*, e58795. https://doi.org/10.7554/eLife.58795

Schenone, S., C., B., F., M., M., R., & M., B. (2011, June 30). *ATP-Competitive Inhibitors of mTOR: An Update*. Current Medicinal Chemistry. https://www.eurekaselect.com/74340/article

Schoof, H., Lenhard, M., Haecker, A., Mayer, K. F. X., Jürgens, G., & Laux, T. (2000). The Stem Cell Population of Arabidopsis Shoot Meristems Is Maintained by a Regulatory Loop between the CLAVATA and WUSCHEL Genes. *Cell*, *100*(6), 635–644. https://doi.org/10.1016/S0092-8674(00)80700-X

Schwarz, I., Scheirlinck, M.-T., Otto, E., Bartrina, I., Schmidt, R.-C., & Schmülling, T. (2020). Cytokinin regulates the activity of the inflorescence meristem and components of seed yield in oilseed rape. *Journal of Experimental Botany*, *71*(22), 7146–7159. https://doi.org/10.1093/jxb/eraa419

Sesma, A., Castresana, C., & Castellano, M. M. (2017). Regulation of Translation by TOR, eIF4E and eIF2α in Plants: Current Knowledge, Challenges and Future Perspectives. *Frontiers in Plant Science*, *8*. https://doi.org/10.3389/fpls.2017.00644

Shi, L., Wu, Y., & Sheen, J. (2018). TOR signaling in plants: Conservation and innovation. *Development*, *145*(13).

Svačinová, J., Novák, O., Plačková, L., Lenobel, R., Holík, J., Strnad, M., & Doležal, K. (2012). A new approach for cytokinin isolation from Arabidopsis tissues using miniaturized purification: Pipette tip solid-phase extraction. *Plant Methods*, *8*(1), 17. https://doi.org/10.1186/1746-4811-8-17

Tafur, L., Kefauver, J., & Loewith, R. (2020). Structural insights into TOR signaling. *Genes*, *11*(8), 885.

Takei, K., Yamaya, T., & Sakakibara, H. (2004). Arabidopsis CYP735A1 and CYP735A2 Encode Cytokinin Hydroxylases That Catalyze the Biosynthesis of trans-Zeatin. *Journal of Biological Chemistry*, *279*(40), 41866–41872. https://doi.org/10.1074/jbc.M406337200

Wang, P., Zhao, Y., Li, Z., Hsu, C.-C., Liu, X., Fu, L., Hou, Y.-J., Du, Y., Xie, S., Zhang, C., Gao, J., Cao, M., Huang, X., Zhu, Y., Tang, K., Wang, X., Tao, W. A., Xiong, Y., & Zhu, J.-K. (2018). Reciprocal Regulation of the TOR Kinase and ABA Receptor Balances Plant Growth and Stress Response. *Molecular Cell*, *69*(1), 100-112.e6. https://doi.org/10.1016/j.molcel.2017.12.002

Wang, X., Ding, J., Lin, S., Liu, D., Gu, T., Wu, H., Trigiano, R. N., McAvoy, R., Huang, J., & Li, Y. (2020). Evolution and roles of cytokinin genes in angiosperms 2: Do ancient CKXs play housekeeping roles while non-ancient CKXs play regulatory roles? *Horticulture Research*, *7*(1), 29. https://doi.org/10.1038/s41438-020-0246-z

Werner, T., Motyka, V., Laucou, V., Smets, R., Van Onckelen, H., & Schmülling, T. (2003). Cytokinin-deficient transgenic Arabidopsis plants show multiple developmental alterations indicating opposite functions of cytokinins in the regulation of shoot and root meristem activity. *The Plant Cell*, *15*(11), 2532–2550.

Xiong, Y., McCormack, M., Li, L., Hall, Q., Xiang, C., & Sheen, J. (2013). Glucose–TOR signalling reprograms the transcriptome and activates meristems. *Nature*, *496*(7444), 181–186. https://doi.org/10.1038/nature12030

Yoshida, S., Mandel, T., & Kuhlemeier, C. (2011). Stem cell activation by light guides plant organogenesis. *Genes & Development*, *25*(13), 1439–1450. https://doi.org/10.1101/gad.631211

Zatloukal, M., Gemrotová, M., Doležal, K., Havlíček, L., Spíchal, L., & Strnad, M. (2008). Novel potent inhibitors of A. thaliana cytokinin oxidase/dehydrogenase. *Bioorganic & Medicinal Chemistry*, *16*(20), 9268–9275. https://doi.org/10.1016/j.bmc.2008.09.008

Zürcher, E., Tavor-Deslex, D., Lituiev, D., Enkerli, K., Tarr, P. T., & Müller, B. (2013b). A Robust and Sensitive Synthetic Sensor to Monitor the Transcriptional Output of the Cytokinin Signaling Network in Planta. *Plant Physiology*, *161*(3), 1066–1075. https://doi.org/10.1104/pp.112.211763

Acknowledgements

We thank Sebastian Wolf and Aurelio Teleman for their ideas and scientific input and Tomas Werner for sharing the p35S:cMyc-CKX1 line. The authors give sincere thanks to Hana Martínková and Petra Amakorová for their help with phytohormone analyses. This work was supported by the ERC grant (#282139) “StemCellAdapt”, the CellNetworks Cluster of Excellence (DFG) and the SFB873 (DFG) to JL, as well as the Ministry of Education, Youth and Sports of the Czech Republic (European Regional Development Fund-Project “Plants as a tool for sustainable global development” No. CZ.02.1.01/0.0/0.0/16_019/0000827).

Author contributions

O.N. and M.S. performed the cytokinin profiling experiment, Y.D. performed the ribosome fractionation experiment and gave input for results interpretation, L.A.R. gave input for results interpretation, A.P. performed one WUS reporter assay generated the cross between the DR line and p35S ARR1∂DDK:GR and designed experiments, D.J. performed all other experiments, designed experiments, curated and analyzed the data, wrote the first draft, revised and edited the manuscript, J.U.L. designed experiments, wrote the final manuscript and acquired the funding.

Figures and legends

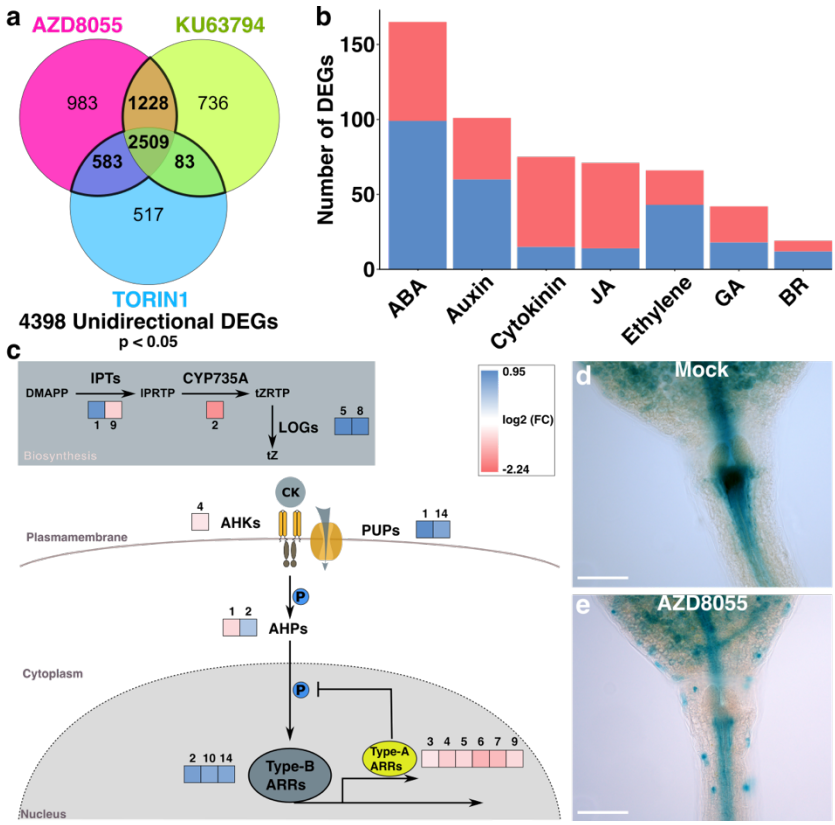

Figure 1: TOR inhibition leads to reduced CK signaling in the SAM

a) Overlaps of differentially expressed genes after treatment with different TOR inhibitors **b)** Gene count of DEGs from RNAseq analysis annotated with hormone signaling function from GO term analysis. ABA = abscisic acid, JA = jasmonic acid, GA = gibberellic acid, BR = brassinosteroids. **c)** Schematic representation of the CK signaling pathway. Color code represents log fold change value obtained by RNAseq. The numbers over the boxes indicate the isoform number of the respective gene. IPT = isopentyltransferase, LOG = lonely guy, AHK = Arabidopsis histidine kinase, AHP = Arabidopsis histidine phosphotransferase, ARR = Arabidopsis response regulator, PUP = purine permease. **d, e)** Representative microscopic images of pTCSn:GUS reporter line treated with either DMSO or AZD8055 for 24 h. Scale bar = 30 μm.

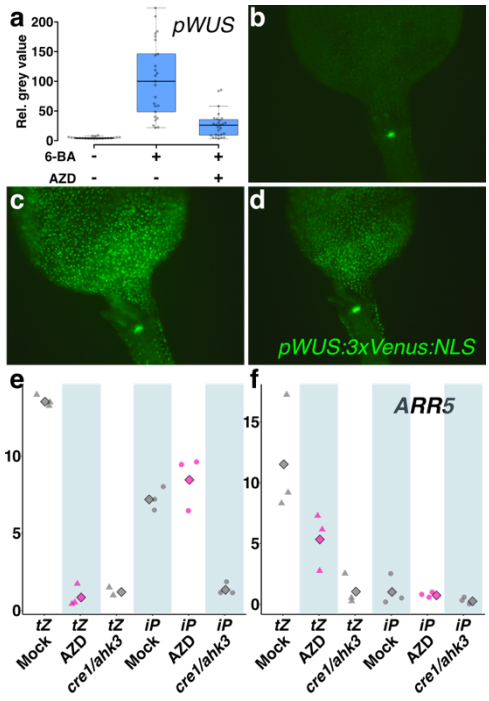

Figure 2: CK output potential is not affected by TOR inhibition

a) Quantification of pWUS:3xVenus:NLS reporter signal of etiolated seedlings treated with 0.5 μM 6-benzyladenine and 2 μM AZD8055 for 3 days. Significant differences between Mock-BA(p=4.05e-13), Mock-BA+AZD (p=5.88e-08) and BA-BA+AZD (p=1.42e-07) were calculated with Wilcoxon rank sum test with Hochberg correction. n=22-27 **b-d)** Representative microscopic images of p35S:ARR1∂DDK:GR crossed with pWUS:3xVenusNLS. Light grown seedlings were treated with b) mock, c) 10 μM dexamethasone (DEX) or d) DEX + 2 μM AZD8055 for 24 h. **e, f)** Relative expression values obtained by q-RT-PCR from e) root and f) shoot. Seedlings were preincubated on AZD8055 or mock for 8h and subsequently treated with either 100 nM trans-zeatin (tZ) or 100 nM isopentyladenine (iP) for 30 min. Data points show expression values from biological replicates (triangles and circles) together with the calculated mean (rhombus).

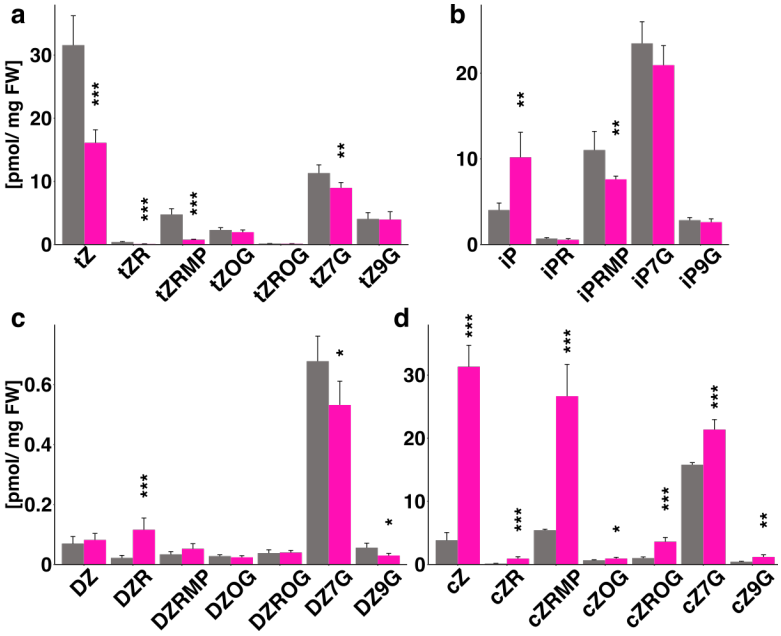

Figure 3: Disturbed CK homeostasis after TOR inhibition

Quantification of different CK species in seedlings treated with AZD8055 (magenta) or mock (grey) for 8 h. Asterisks indicate significant differences of the AZD8055 treated sample compared with the respective mock control calculated with two-tailed t-test (*, **, and *** correspond to P-values of $0.05 > p > 0.01$, $0.01 > p > 0.001$, and $p < 0.001$, respectively). Error bars indicate standard deviation. n =5. **a)** tZ = trans-zeatin, tZR = trans-zeatin riboside, tZRMP = trans-zeatin riboside-5´monophosphate, tZOG = trans-zeatin O-glucoside, tZROG = trans-zeatin riboside O-glucoside, tZ7G = trans-zeatin-7-glucoside, tZ9G = trans-zeatin-9-glucoside **b)** iP = isopentyladenine, iPR = isopentyladenosine, iPRMP = isopentyladenosine-5´monophosphate, iP7G = isopentyladenine-7-glucoside, iP9G = isopentyladenine-9-glucoside **c)** DZ = dihydrozeatin, DZR = dihydrozeatin riboside, DZRMP = dihydrozeatin riboside-5´monophosphate, DZOG = dihydrozeatin O-glucoside, DZROG = dihydrozeatin riboside O-glucoside, DZ7G = dihydrozeatin-7-glucoside, DZ9G = dihydrozeatin-9-glucoside **d)** cZ = cis-zeatin, cZR = cis-zeatin riboside, cZRMP = cis-zeatin riboside-5´monophosphate, cZOG = cis-zeatin O-glucoside, cZROG = cis-zeatin riboside O-glucoside, cZ7G = cis-zeatin-7-glucoside, cZ9G = cis-zeatin-9-glucoside

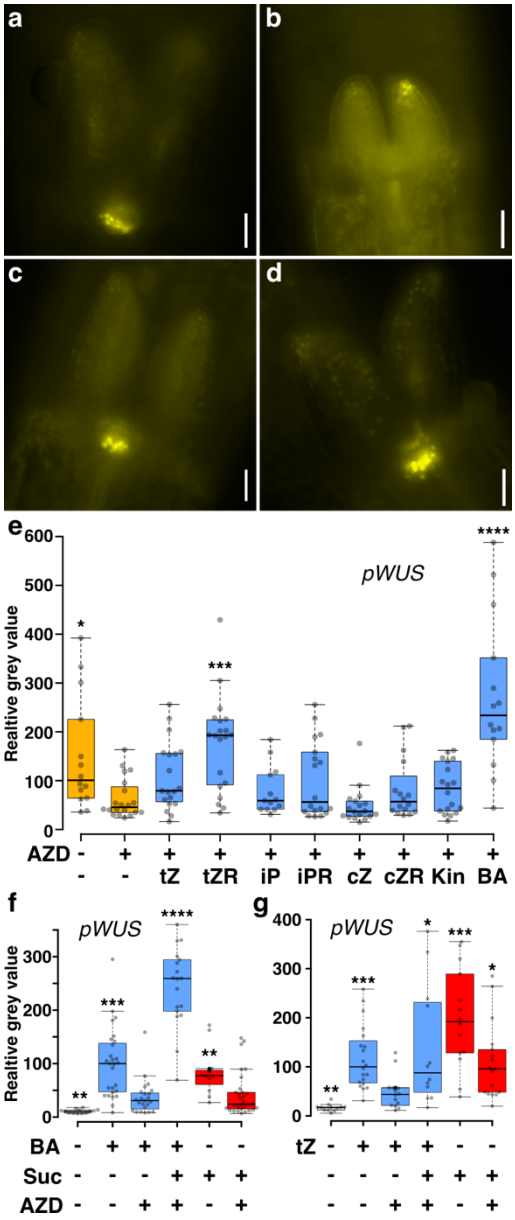

Figure 4: trans-zeatin species rescue *WUS* expression after TOR inhibition

Representative microscopic images of pWUS:3xVenus:NLS reporter line treated with **a)** mock **b)** 2μ AZD8055 **c)** AZD + 0.5 μM tZR and **e)** AZD + 0.5 μM 6-BA. Images were acquired as black and white and false color coded with imagej. Scale bar = 30 μm. **e)** Quantification from a)-d) of pWUS:3xVenus:NLS reporter signal. Light grown seedlings were treated with 2 μM AZD8055 and 0.5 μM of different CK species for 1 day. Asterisks indicate significant differences compared to the AZD treated conditions. n=13-20. **f, g)** Quantification of pWUS:3xVenus:NLS reporter signal. Etiolated seedlings were treated with 0.5 μM 6-benzyladenine (BA) or trans-zeatin (tZ), 2 μM AZD8055 and/or 1% sucrose for 3 days in the dark. Asterisks indicate significant differences compared to the BA+AZD or tZ+AZD condition. **f)** n=13-30 **g)** n=12-20. Significance levels were calculated using the Wilcoxon rank sum test

with Hochberg correction (* = $p < 0.05$; ** = $p < 0.01$;*** = $p < 0.001$, **** = $p < 0.0001$). tZ = trans-zeatin, tZR = trans-zeatin riboside, iP = isopentyladenine, iPR = isopentyladenosine, cZ = cis-zeatin, cZR = cis-zeatin riboside, Kin = kinetin, BA = 6-benzyladenine.

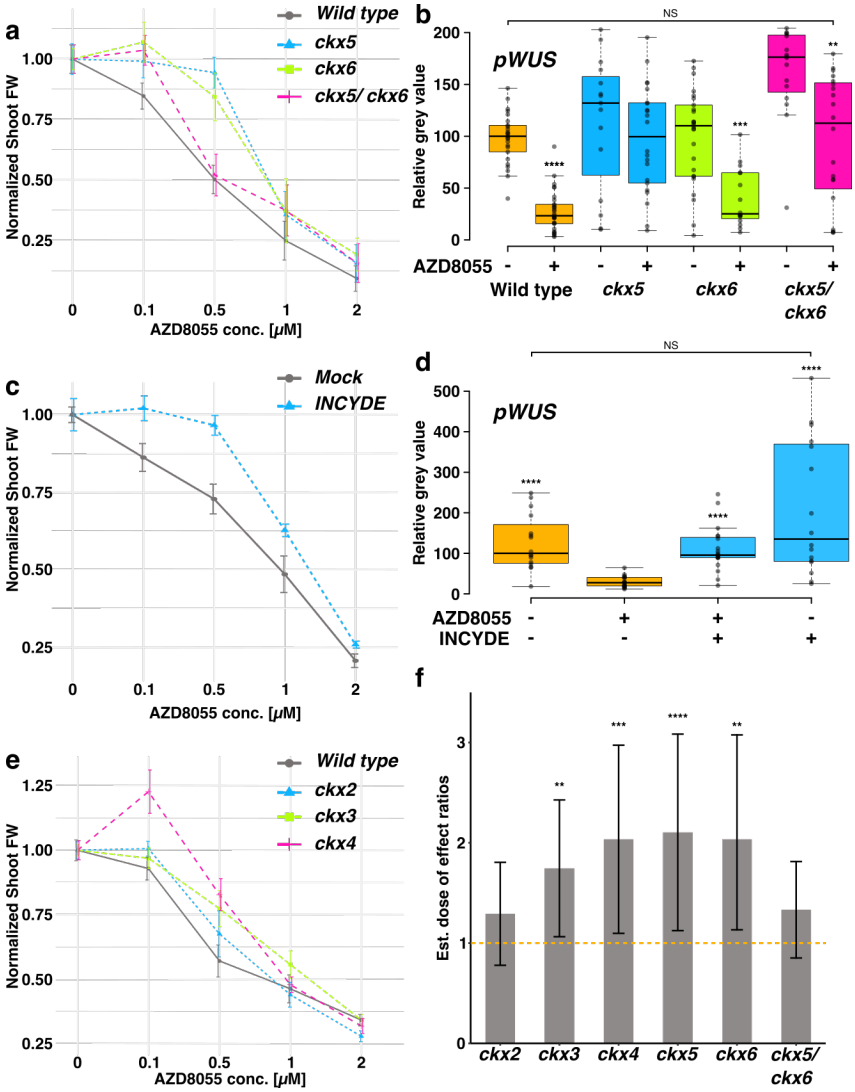

Figure 5: Specific *CKX* mutations confer resistance to TOR inhibition

a, c, e) Average shoot fresh weight per seedling 7 days after transfer to AZD8055 plates containing. Data for each measurement was derived from ~40 seedlings from two independent experiments and normalized to untreated average. Error bars represent standard error. Plots of raw data is shown in the supplements. Significant interaction was tested before normalization with ANOVA linear mixed effect models (Freshweight ~ AZDconc.*Genotype + (1|Experiment) for a) p = 0.00014 e) p = 6.87e-08 and for c) p = 0.0123. Pairwise comparisons are found in the supplements **a)** *ckx5*, *ckx6* and *ckx5/6* are in the genetic background of *pWUS:3xVenusNLS*, *pCLV3:mCherry:NLS* and were tested against this background. **c)** 75 nM INCYDE. **b, d)** Quantification of pWUS:3xVenus:NLS reporter signal. Seedlings were grown in the light for 3 days and treated with mock, 2 µM AZD8055 and/ or 75 nM INCYDE for 1 day. **b**) Asterisks indicate significant differences between the AZD treated condition and the respective Mock. n=15-29 **d)** Asterisks indicate significant differences compared to the

AZD treated condition. n=16-19. For b) and d) Significance levels were calculated using the Wilcoxon rank sum test with Hochberg correction **f)** Estimated dose of effect ratios comparing ED50 values of different ckx mutants with the respective wild type background. Error bars indicate 95% confidence intervals. Orange dashed line indicates the wild type reference level which is set to 1. Asteristks indicate significantly different ED50 calculated with ANOVA. (* = $p < 0.05$; ** = $p < 0.01$;*** = $p < 0.001$, **** = $p < 0.0001$).

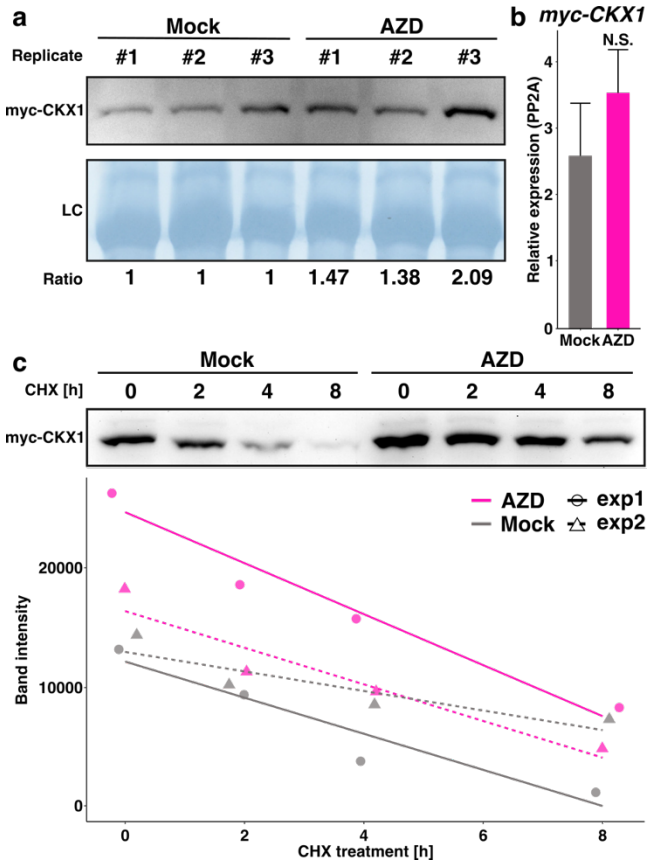

Figure 6: cMyc-CKX1 protein accumulates after TOR inhibition

a) Western blot of p35S:cMyc-CKX1 seedlings treated with either mock or 2μM AZD8055 for 8h. Shoot protein extract was probed with anti-cMyc serum. Replicates are from three independent experimental repetitions. Loading control (LC) stained with amido black. Ratios were calculated between band intensities from myc-CKX1 signal and the LC and normalized against the respective mock sample. **b)** q-RT-PCR of p35S:cMyc-CKX1 shoots with primers against the transgene transcript. No significant difference using two biological replicates was found using paired t-test (p=0.3). Error bars represent standard deviation. **c)** Western blot of p35S:cMyc-CKX1 shoot protein extract probed with anti cMyc serum. Seedlings were pre-incubated on AZD8055 and then flooded with 200 μM cycloheximide solution for the indicated time. Band intensities from two independent experimental repetitions were plotted with linear regression lines.

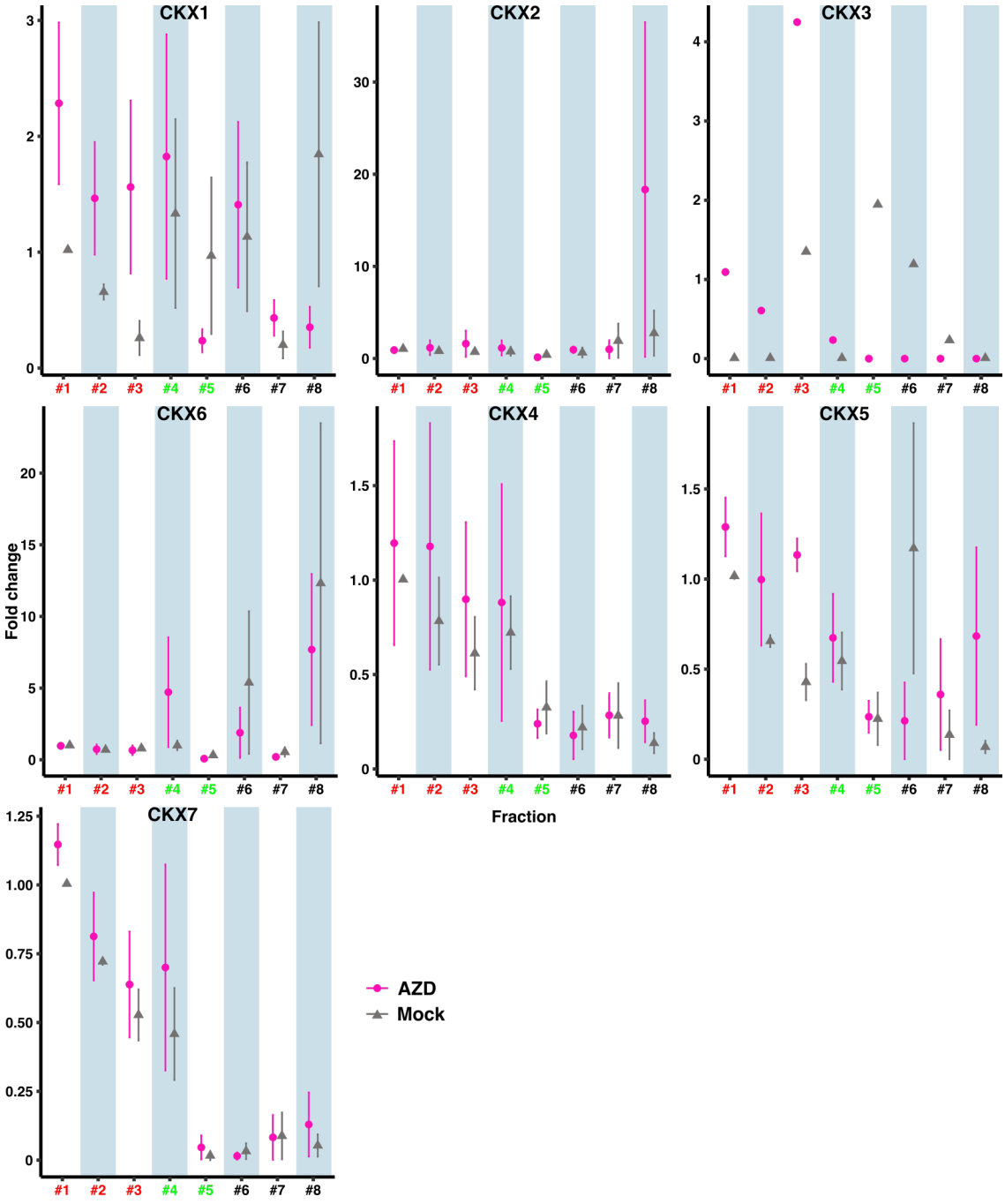

Figure 7: Translation of specific CKX transcripts is repressed by TOR

CKX mRNAs were quantified in ribosomal fractions by q-RT-PCR relative to *UBI10* and normalized to the respective mock of fraction #1. Error bars represent standard error of the mean of data pooled from three independent experimental repetitions (except CKX2 and CKX7 only detected in 2 replicates, CKX3 was detected in 1 replicate). Red numbers indicate heavy polysomal fractions (fractions 1-3), green numbers light polysomal fractions (fractions 4+5) and black number monosomal fractions (fractions 6-8). Individual data points are shown in the supplements (Fig. S18).